

STUDY OF THE SiO₂ PLASMA PHYSICAL PARAMETERS: TEMPERATURE, ELECTRON DENSITY, PRESSURE, RADIATION

Bussière William⁽¹⁾, Rochette David⁽²⁾ and André Pascal⁽³⁾

LAEPT CNRS UMR 6069⁽¹⁾, Phys. Bât. 5 – 24, Av. des Landais – F63177 AUBIERE CEDEX FRANCE, william.BUSSIÈRE@laept.univ-bpclermont.fr
 LAEPT CNRS UMR 6069^(2,3), Phys. Bât. 5 – 24, Av. des Landais – F63177 AUBIERE CEDEX FRANCE, david.ROCHETTE@laept.univ-bpclermont.fr⁽²⁾, pascal.ANDRE@laept.univ-bpclermont.fr⁽³⁾

Abstract: During the fault current breaking process in a fuse, the energy brought by the electric current implies the fusion and the vaporization of the fuse element and the filler (usually silica sand). Consequently a plasma is created. The plasma consists of metallic and silicon. We use the radiation escaped from the plasma to measure the plasma temperature and the electron density. The results are given for different mean granulometry and packing density, and compared with other experimental results obtained from the literature. Moreover, for modelling purpose, the measurements are compared with theoretical calculation (thermodynamic properties) to deduce the valid assumptions.

Keywords: Plasma, atomic spectroscopy, Stark broadening, Helmholtz free energy minimisation, composition, electron density, pressure.

1. Introduction

Within the framework of research areas concerning fault current breaking devices, especially H.B.C. fuse, researchers are interested with the evolutions of the physical parameters of the plasma, namely the plasma temperature (T) [1-2], the electron density (n_e) [3-5], the pressure (P) [6]. These properties are linked to fundamental parameters, such as the electrical conductivity, the thermal conductivity, the transport coefficients which are necessary to establish realistic modelling.

Once the fuse plasma is initiated, the dissipated energy is responsible for the fuse element and silica sand fusion and vaporization. Thus the plasma volume varies according to the energy brought by the electric current and the ability of the filler to withdraw the energy from the plasma to the surroundings. In Section 2, we give a quick depiction of the experimental set-up used to collect the radiation escaped from the plasma, and the n_e/T characteristics measured for different morphometric properties of the silica sand. In Section 3, we briefly recall the hypothesis, the physical formulation and the calculation method concerning electron density, pressure and spectral line intensity. In Section 4, the two types of results are compared.

2. Temperature and electron density measurement

2.1. Test fuse and test circuit

The test fuse is designed to reproduce the breaking phenomenon of an industrial fuse. We use a single silver fuse element with two notches. The front side of the test fuse consist of a quartz window designed to collect the light issued from the plasma. The fuse strip is set in such a way that only the section of the fuse strip is in contact with the quartz window. Thus the interaction between the plasma and the window is

reduced, and the fulgurite obtained after the fuse working is similar to those obtained in an industrial fuse. The cavity is filled with silica sand grains. The mean granulometry and packing density are controlled before the test.

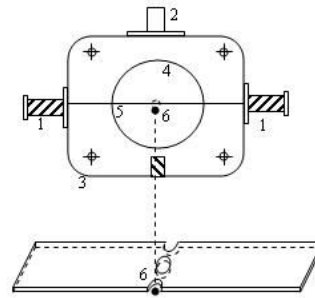


Fig. 1: Test fuse. 1, metal electrodes ; 2, cavity obturator ; 3, cartridge ; 4, filling cavity ; 5, fuse strip ; 6, observation point.

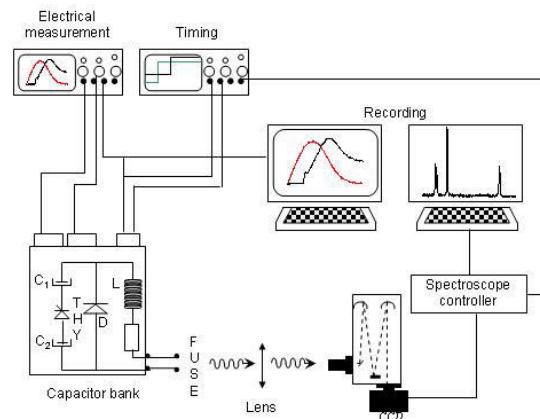


Fig. 2: Schematic diagram of the test set-up.

The energy is delivered by means of a capacitor bank discharge: the short-circuit prospective current is 3.2 kA, and the stored voltage is 460 V. The frequency of the waveforms of the current through and the voltage across the fuse is about 50 Hz. A 416 A.V⁻¹ current shunt and 100 V.V⁻¹ voltage shunt are used to measure the current through and the voltage across the fuse. The start of the capacitor bank discharge is synchronized with the emission of the radiation escaped from the plasma. Typical electrical measurements can be found in [7].

The fuse filler is silica sand of high purity (99.80%). Various mean granulometry and packing densities are used (Table 1).

Table 1. Characterization of the silica sand. Each of the granulometric intervals is 50 μm wide. Each of the packing density letter represents 0.04 g.cm⁻³. The first letter represents the smallest value for the two parameters.

Parameter	Value
Real density (g.cm ⁻³)	2.65
Apparent density (g.cm ⁻³)	1.50
Granulometric intervals	A, B, C, D, E, F, G
Packing density	a, b, c, d, e, f

2.2. Collection of the plasma radiation

The radiation issued from the plasma is collected via an optic fibre plus lens system and focussed to the entrance slit of the spectroscope. The used spectroscope is a Chromex 500 IS, 500 mm-focal length. We use two diffraction gratings, a 1200-gr.mm⁻¹ and 1800-gr.mm⁻¹ grating, which correspond to the respective spectral range ~ 45 nm and ~ 25 nm. The spectrum is recorded by means of a CCD matrix (size in pixel: 1242×1152) used in a kinetic mode which allows to obtain many tracks equally distributed throughout the whole duration of the plasma radiation emission. A viewing of the maximum and minimum intensity of each track is given in Fig. 3 together with the electric power evolution during the fuse working. The radiation intensity depends directly to the electric power level: immediately after the arc ignition corresponding to the voltage drop (~ 0.9 ms), the radiation intensity quickly increases such as the electric power. At the decrease of the electric power, the radiation intensity gradually decreases until 4 ms. Once the electric power is zero, the radiation can not be used any more.

Two spectral intervals are studied in order to evaluate the temperature and the electron density. For both evaluations, we used the ionized silicon lines whose spectroscopic properties are in given in Table 2.

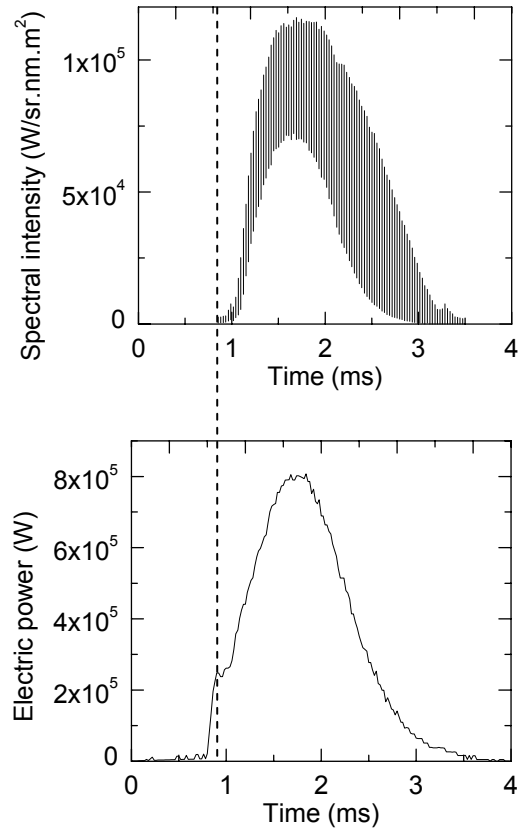


Fig.3: Evolution of the radiation profile for the spectral interval focussed on 635 nm and the electric power for the prearcing plus arcing time.

Table 2. Configurations of the two kinetic modes used for the study of the plasma radiation.

Total duration of a track (ms)	0.038	0.022
Number of tracks	94	143
Total time (ms)	~ 3.6	~ 3.1

2.3. Temperature measurement

The temperature is obtained from the ratio of two spectral line intensities issued from the same ion species, assuming that the Boltzmann distribution of the energy levels is valid. The temperature is given by:

$$T = \frac{E_{u1} - E_{u2}}{k_B} \times \frac{1}{\log \left(\frac{\lambda_{ul,2} g_{u1} A_{ul,1}}{\lambda_{ul,1} g_{u,2} A_{ul,2}} \times \frac{J_2}{J_1} \right)}$$

where the subscript 1 and 2 correspond to the two spectral lines, λ_{ul} is the central wavelength, g_u is the statistical weight of the upper energy level E_u ,

Table 2. Spectroscopic properties of the ionized silicon lines used for the evaluation of the temperature and the electron density [8].

Multiplet	Theoretical wavelength (nm)	Upper energy level (eV)	Statistical weight	Transition probability (10^8 s^{-1})	Theoretical intensity ratio within multiplets (LS coupling) [9]
1	385.602	10.073883	4	0.25	1.78
	386.259	10.066447	2	0.28	
2	634.711	10.073883	4	0.70	2.00
	637.137	10.066447	2	0.69	
3	413.089	12.839316	8	1.32	1.43
	412.805	12.839332	6	1.42	

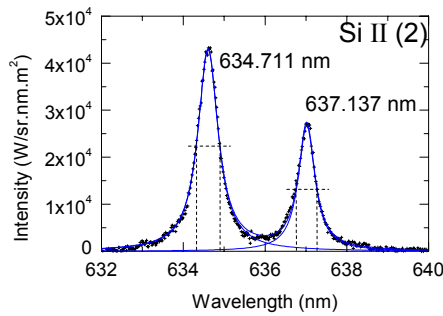


Fig. 4: Fit of the experimental Si II (2) multiplet line profiles (+). The full curves represent the fitted profile from which the HWHMs are deduced. This spectrum is observed at the end of the fuse working (~ 3.5 ms).

A_{ul} is the transition probability, and J is the total area of the spectral line. The difference in energy between the upper energy levels of the two lines must be 2 eV at least. To reduce the possible errors in the intensity calibration, we choose two ionized silicon lines visible in the same spectral interval. The total areas J are fitted for each of the tracks, and for the four lines corresponding to the multiplets 1 and 3. Thus we express four temperature values for each track. We use the total area rather than the maximal intensity because the corresponding line profile is due to some broadening processes resulting from the plasma parameters (density, temperature, pressure). We have to notice that the light escaped from the plasma is integrated on an unknown thickness. Thus the resulting temperature is not a local value.

2.4. Electron density measurement

Many processes can be responsible for the broadening of the spectral line. We can distinguish the broadening due to the collisions of the radiating species with neutral particles (natural, Doppler, Van der Waals broadenings), and the broadening due to

the collisions with charged particles (Stark effect mainly). The first type of broadening is not significant in the case of the fuse plasma. The resulting Half Width at Half Maximum (HWHM) is clearly less than one nanometre. On the contrary, the local electric strength in the fuse plasma implies the splitting of the radiating energy level, and thus the broadening of the spectral line profile. The resulting HWHM can be several nanometres. The ionized silicon Half HWHM due to the Stark effect is tabulated in the literature for various temperature and electron density values [10]. Considering that the electron impact HWHM varies linearly with the electron density (the dependence with the temperature is weak) we can deduce the electron density in the fuse plasma from the experimental HWHM. This processing is valid as long as the lines are isolated, such as the Si II (3) lines. But in the fuse, the plasma core is surrounded by cold layers responsible for the radiation absorption. This implies a supplementary broadening which can not be differentiated from the Stark broadening. Consequently, the electron density deduced from the Si II (3) HWHM can be overestimated.

2.5. Electron density versus temperature characteristics for different morphometric properties

In order to compare the measurements with the calculations, we represent the electron density versus temperature for various values of the granulometry and packing density of the silica sand. The results are given in Fig. 5 for six consecutive granulometric intervals, each of them being $50 \mu\text{m}$ -wide.

The number of measurements is linked to the granulometry. Smaller the granulometry, smaller the number of valid spectrums can be observed. On the full temperature range investigated, it is not possible to fit the experimental profiles for temperature higher than 17 000 K. The measurements corresponding to this temperature range show a decreasing electron density with increasing temperature. From the experimental point of view, it may be explained by the absorption of the radiation escaped from the

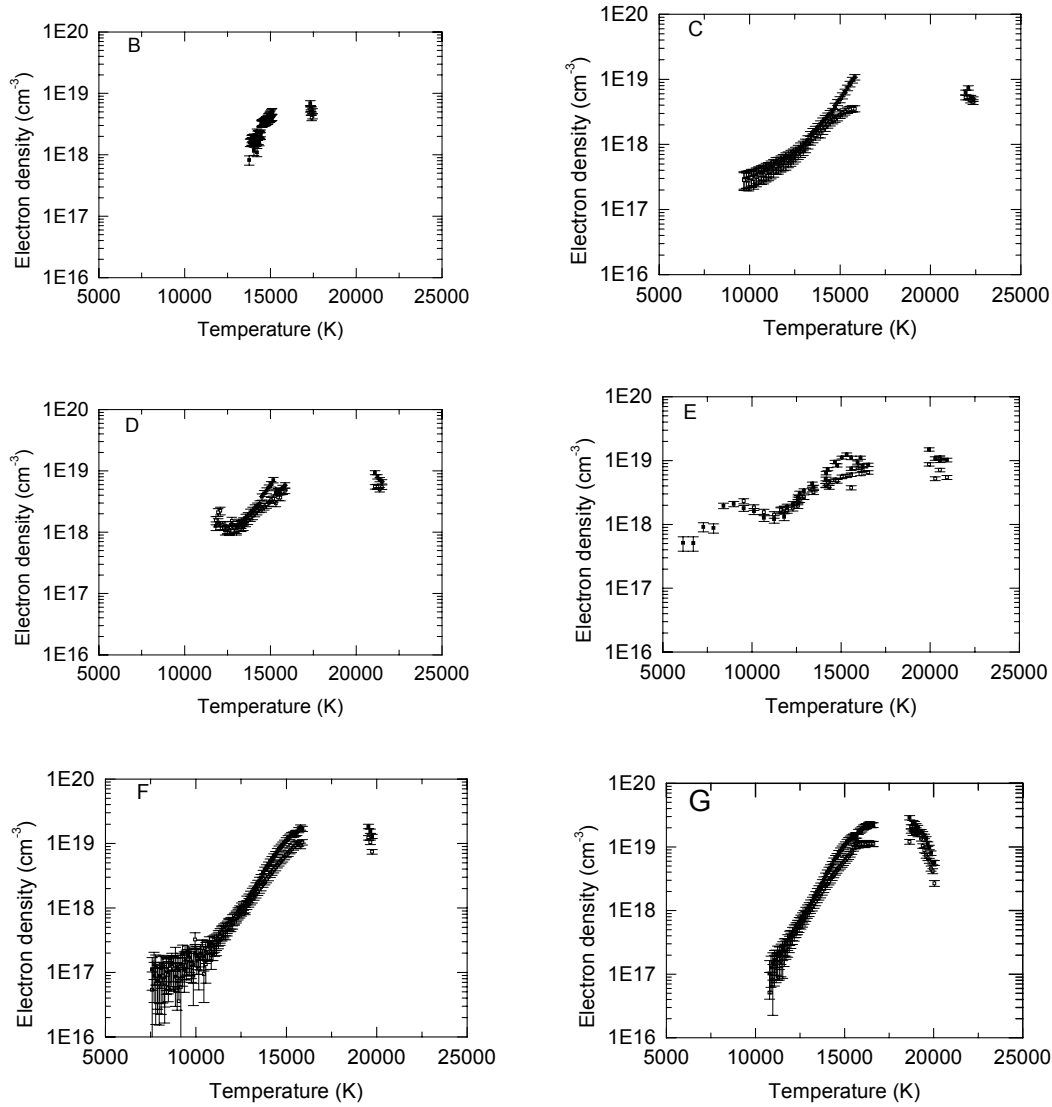


Fig. 5: Electron density versus temperature for the increasing 50 μm -granulometric intervals B, C, D, E, F, G.

inner part of the plasma by the cooler surrounding layers. Thus, the ionized silicon line profile is broadened by absorption, and the fitted HWHM is the combination of the two broadening processes, Stark broadening and absorption broadening. From This is linked to the dissipated energy, the $I^2.t$, the electric power which vary in function of the morphometric properties. Whatever the parameter, the variation is significant: the temperature varies between 22 000 K and 10 000 K, and the electron density varies between 10^{16} cm^{-3} and 10^{19} cm^{-3} . To measure the temperature and the electron density, we observe the plasma radiation in two different spectral domains that can not be studied simultaneously with a single acquisition. Thus, in Fig. 5, the temperature is the value deduced from the acquisition realized in a different spectral domain than those observed for the electron density measurement.

the electron density versus temperature characteristics, there is no significant discrepancy between the different granulometries, except for the smallest temperatures.

3. Calculation applied in the case of a SiO_2 plasma

In a purpose to determine theoretically the electronic density number, the pressure and the intensity of monatomic spectral lines versus temperature and for various densities, we have made a calculation code. This calculation code is based on the minimisation of Helmholtz free energy that allows us to determine the plasma composition versus temperature for a fix plasma density. With the Dalton law we calculate the pressure versus temperature. Then for the interesting chemical species (Si^+), by assuming a Boltzmann distribution on excitation

level we calculate the spectral line intensities versus temperature [11].

In our calculation code, we take the following chemical species into account: e^- , O , O^- , O^+ , O^{++} , O^{+++} , Si , Si^- , Si^+ , Si^{++} , Si^{+++} , O_2 , O_2^- , O_2^+ , Si_2 , SiO , O_3 , Si_3 , SiO_2 .

We have to notice that the calculation is made only with silica. As a matter of fact since the comparison is made after the creation of plasma between the two silver electrodes and since the thermal conductivity of liquid and solid silver is higher than for the silica. The diffusion of heat is made quicker for silver than for silica. So, the vaporisation is higher for silica than for silver [12] and consequently in a simplification purpose we consider a plasma formed in silica vapours in our calculation.

4. Discussion

As a first step, we compare the intensity of the ionized silicon lines versus temperature in so far as these lines are used in the diagnostic (Fig. 6). Second, we compare the profiles of the pressure measured inside the filler with the profiles obtained from the simulation and the calculation (Fig. 7). Third, we compare the electron density versus temperature characteristics (Fig. 8).

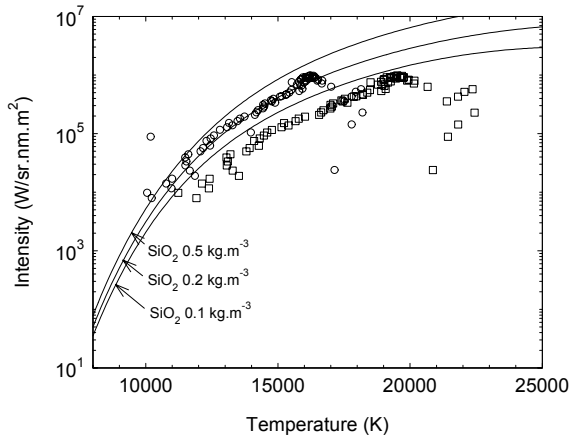


Fig. 6: Comparison of the observed intensity of the Si II (1) 385.602 nm line with the calculation at constant volume for three initial densities of silica. ○, temperature scale 1 ; ◻, temperature scale 2.

The evolution of the Si II (1) 385.602 nm line versus temperature is given in Fig. 6 for two experimental temperature scales. These temperature scales are deduced from the Si II (1) and Si II (3) lines areas. For each track, four values are fitted from which we express two mean trends, symbolized 1 and 2 in Fig. 6. We observe that the experimental points follow the calculated curves for a given SiO_2 initial density. For the higher temperatures, the experimental points clearly deviate from the

calculated curves. Two main reasons can justify this discrepancies.

- First, at the beginning of the arcing time, the plasma is made of silver and silicon. The relative proportion of the two species is very difficult to determine. But a few percentage of silver can strongly influences the silicon lines intensity.

- Second, the radiation absorption due to the cold surroundings can strongly affects the spectral line area. Moreover, the radiation absorption depends on the wavelength and it can be different for the Si II (1) and Si II (3) multiplets.

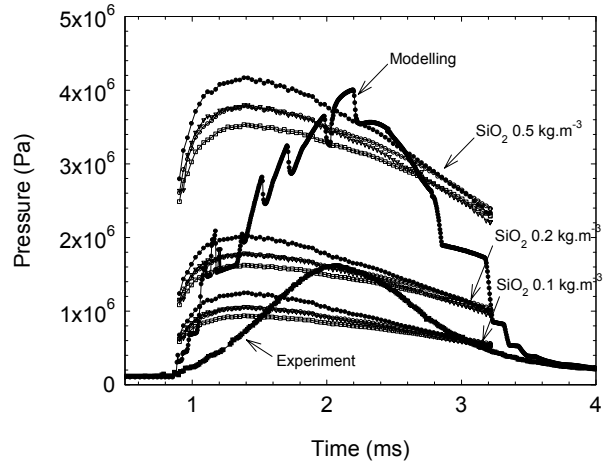


Fig. 7: Evolution of the pressure versus time. We report the SiO_2 plasma pressure calculated at constant volume for three initial densities, the pressure in the arc core obtained with modelling [13], and the pressure measured inside the filler at the immediate vicinity of the fulgurite.

Taking into consideration the evolution of the Si II (1) and Si II (3) lines intensity on one side, and the calculation on the other side, we can deduce the corresponding plasma pressure for a given density and temperature. Then, the plasma pressure is expressed as a function of time. The deduced pressure is compared in Fig. 7 with the pressure obtained from modelling and with the pressure measured in the filler, at the vicinity of the fulgurite. The experimental pressure can be interpreted as the low limit of the plasma core pressure. Three results can be expressed.

- First, the experiment and the modelling give coherent results ; the curves are similar for the increase and the decrease of the pressure. The maximum is different: $\sim 40 \cdot 10^5$ Pa for modelling, $\sim 16 \cdot 10^5$ Pa for experiment ; this discrepancy is logical in so far as we compare the plasma pressure with the pressure inside the filler. The plasma pressure is transmitted to the granular filler via the surroundings of the fuse plasma. These surroundings consist of different layers, mainly liquid and eroded sand grain

resulting from the flow of vapour from the plasma core [14].

- Second, the two maximums are nearly observed simultaneously, and they correspond to the maximum of the electric power. On the whole duration of the fuse working, the evolution of the pressure is nearly the same as the evolution of the electric power.

- Third, the pressure deduced from the Si II spectral lines intensity and the calculation do not show a logical evolution versus time. In fact, the calculation is performed for a given density ; due to the closeness of the plasma with the sand grains, we can suppose that some silicon vapours are produced while the energy is sufficient. If the energy decreases, the density of the plasma should decrease too. Thus the plasma pressure has to be calculated using different initial densities to describe the whole duration of the fuse working.

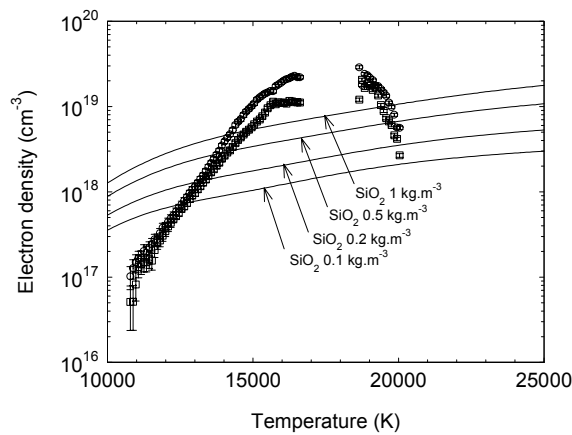


Fig. 8: Comparison between the experimental electron density and the calculation at constant volume for various initial densities.

The electron density number deduced from the Si II (2) multiplet HWHMs is given versus temperature in Fig. 8 together with the calculated evolution with corresponding initial density.

- The electron density number logically increases for the temperature range from $\sim 10\,000$ K to $\sim 17\,000$ K. This trend is similar to the calculated curves. For the temperature range from $\sim 17\,000$ K to $\sim 19\,000$ K, the Si II (2) multiplet line profile can not be fitted any more. The spectral lines are broadened by absorption, and the continuum (Bound-free and free-free radiation) becomes more intense than the discrete radiation. For the temperature range from $\sim 19\,000$ K to $\sim 22\,000$ K, the electron density number decreases. This is opposite to the calculation. This error can be due to the absorption: first the absorption implies a broadening of the Si II (2) multiplet line profile ; second, the temperature deduced from the Si II (1) and Si II (3) multiplets can be overestimated.

- The experimental points can not be described by a calculation with a single initial density. The experimental curve corresponds successively to different plasma states resulting from increasing initial density. Thus, the difficulty is to define the duration of one state defined by a given density.

5. Conclusion

The physical and thermodynamic properties of the H.B.C. fuse plasma are studied using experiment and theoretical calculations. The two approaches are necessary to give an estimation of the parameters used in the modelling.

By studying the plasma radiation, we estimate the ne/T characteristics. These trends are compared with the calculations assuming a constant volume and a given initial density in the case of a SiO_2 plasma. The comparison of the experimental and calculated Si II lines intensity allows the estimation of the initial density. The corresponding calculated pressure is more difficult to interpret ; it seems obvious that, due to the electrical energy injection on one side, and the plasma energy withdraw linked to the sand properties on the other side, the calculation can not be performed for a single value of the initial density. The evolution of the density used in the calculation has to be determined in the future to give the necessary information for the modelling.

Acknowledgements

We thank, both for their financial support and their help through many discussions, M. S. Melquiond and T. Godechot from Alstom, M. V erit e from E.D.F, M. T. Rambaud and J.L. Gelet from Ferraz-Shawmut, and M. C. Fi evet and F. Gentils from Schneider Electric.

References

- [1] Saquib M.A., Stokes A.D., James B.W., Falconner I.S., "Arc temperature measurement in a high-voltage fuse", ICEFA Turin 1999, p.107.
- [2] Bussiere W, Bezborodko P., "Measurement of time-resolved spectra of fuse arcs using a new experimental arrangement", J. Phys. D: Appl. Phys., 32, pp. 1693-1701.
- [3] Saquib M.A., Stokes A.D., James B.W., Falconner I.S., "Measurement of electron density in a high-voltage fuse arc", ICEFA Turin 1999, p.129.
- [4] Chikata T., Ueda Y., Murai Y., Miyamoto T., "Spectroscopic observations of arcs in current limiting fuse through sand", ICEFA Liverpool 1976, p. 114.

- [5] Bussière W., "Influence of sand granulometry granulometry on electrical characteristics, temperature and electron density during high-voltage fuse arc extinction", *J. Phys. D: Appl. Phys.*, **34**, pp. 935-935.
- [6] Saquib M.A., Stokes A.D., Seebacher P.J., "Pressure inside the arc channel of a high-voltage fuse", ICEFA Turin 1999, p.83.
- [7] Bussière W., Rochette D., Pellet R., "Influence of the filling material properties on pressure. Comparison between experimental results and simulation", ICEFA Gdansk, 2003.
- [8] NIST Database 61, Database for Atomic Spectroscopy (DAS) 1995 National Institute of Standards and Technology, <http://aeldata.phy.nist.gov/archive/el.html>.
- [9] Lesage A., Rathore R.A., Lakicevic I.S., Puric J., "Stark widths and shifts of singly ionized silicon spectral lines", *Phys. Rev. A*, **28**, pp. 2264-2268.
- [10] Griem H.R., "Spectral line broadening by plasmas", New York: Academic Press, 1974.
- [11] Bussière W., André P., "Evaluation of the composition, the pressure, the thermodynamic properties and the monoatomic spectral lines at fixed volume for a SiO₂-Ag plasma in the temperature range 5000-25000 K", *J. Phys. D: Appl. Phys.*, **34**, pp 1657-1664, 2001.
- [12] Lefort A., Abbaoui M., André P., Private communication.
- [13] Rochette D., Clain S., "Numerical simulation of Darcy and Forchheimer force distribution in a H.B.C. fuse", *Transport in Porous Media*, **53**, pp. 25-37, 2003.
- [14] S. Gnanalingam, R. Wilkins, "Digital simulation of fuse breaking tests", *IEE Proc.*, Vol. 127, Pt. C, N°6, November 1980.